

Whole-body imaging with fluorescent proteins

Robert M Hoffman & Meng Yang

AntiCancer, Inc., 7917 Ostrow Street, San Diego, California 92111, USA. Correspondence should be addressed to R.M.H. (all@anticancer.com).

Published online 2 November 2006; doi:10.1038/nprot.2006.223

The intrinsic brightness of fluorescent proteins has been taken advantage of to develop a technology of whole-body imaging of tumors and gene expression in mouse internal organs. Stable transformation with fluorescent protein genes can be effected using retroviral vectors containing a selectable marker such as neomycin resistance. The cells that stably express fluorescent proteins can then be transplanted into appropriate mouse models. For whole-body imaging, nude mice are very appropriate. If wild-type mice are used, then hair must be removed by shaving or depilation. The instruments used can range from a simple LED flashlight and appropriate excitation and emission filters to sophisticated equipment such as the Olympus OV100 with a wide range of magnification, enabling both macroimaging and microimaging. It is crucial that proper filters be used such that background autofluorescence is minimal. Fluorescent protein-based imaging technology can be used for whole-body imaging of fluorescent cells on essentially all organs. The timeline for these experiments varies from 2 days to 2 months.

INTRODUCTION

This protocol enables the user to perform whole-body imaging of fluorescent protein-expressing cells in mouse internal organs (Figs. 1,2) as well as other small animals. The technique has many applications, including visualizing cancer growth and metastasis, gene expression, infectious disease, stem cells, immunology, neurobiology and numerous others. This protocol will focus on cancer and gene expression. A crucial point is the stable expression of fluorescent proteins in the cells to be imaged. Such stable expression can be effected by appropriate vectors containing the fluorescent protein gene and a selectable marker such as antibiotic resistance. A number of green fluorescent proteins (GFP) and red fluorescent proteins (RFP; Fig. 3) are now available for *in vivo* imaging. A wide range of instrumentation can be used for fluorescent protein-based imaging, ranging from an LED flashlight and appropriate excitation and emission filters to highly specific instrumentation such as the Olympus OV100, a small animal imaging apparatus with variable magnification from macro to micro. The technology requires incident excitation light as well as detection of fluorescence emission.

Many different types of cancer models can be used for whole-body imaging, including orthotopic, colon¹, prostate², pancreas³, bone⁴, brain⁵ and other cancer models⁶. The relative transparency of the footpad reduces the scatter of fluorescent light emitted from the tumor, and the relatively few resident blood vessels makes it an excellent tumor transplantation site for whole-body tumor angiogenesis imaging⁷. Many applications of GFP whole-body imaging have already been made to non-invasively visualize cancer^{6,8,9}, gene expression¹⁰, graft vs. host disease¹¹ and infectious disease¹² in animal models.

Estimating the intensity of GFP fluorescence is complicated by variations in the exciting illumination with time and across the imaging area. These factors are corrected for by using the intrinsic red fluorescence of mouse skin as a baseline to correct the increase over intrinsic green fluorescence due to GFP¹⁰. This can be done because there is relatively little red luminance in the GFP radiance. Consequently, the green fluorescence is calculated relative to red based on red and green channel composition in the skin images¹⁰. Therefore, some limits might occur when only a few cells are present in or on a deep organ. These limits can be readily overcome by using skin-flap techniques¹³.

The GFP approach has several important advantages over other optical approaches to imaging tumor growth *in vivo*. In comparison with the luciferase reporter, GFP has a much stronger signal, and therefore can be used to image unrestrained animals — irradiation with non-damaging blue light is the only step needed. Images can be

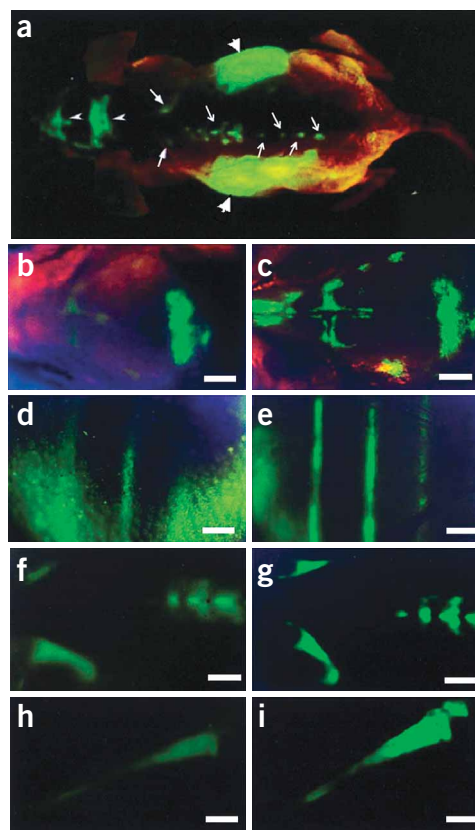


Figure 1 | Comparison of external and internal images of bone metastasis. (a) External images of tumors in the skeletal system including the skull (small arrowheads), scapula (thick arrows), spine (fine arrows), and liver metastasis (hollow arrowheads) in a dorsal view of a live, intact nude mouse. (b–i) Images of the exposed skeletal metastases. Bars, 1280 μm^1 .

PROTOCOL

captured with fairly simple apparatus, and there is no need for total darkness. The fluorescence intensity of GFP is strong^{14–17} and the protein sequence of GFP has also been ‘humanized’, which enables it to be highly expressed in mammalian cells¹⁸. Importantly, unlike luciferase, fluorescent proteins come in a multitude of colors¹⁹, allowing for multiple events to be imaged. In addition, GFP fluorescence is relatively unaffected by the external environment, as the chromophore is protected by the three-dimensional structure of the protein²⁰. A triple fusion reporter vector harboring a *Renilla* luciferase reporter gene, a reporter gene encoding a monomeric RFP, and a mutant herpes simplex virus type thymidine kinase was tested *in vivo*. A highly sensitive cooled charge-coupled device (CCD) camera that is compatible with both luciferase and fluorescence imaging compared these two signals from the fused reporter gene using a lentivirus vector in 293T cells implanted in nude mice. The signal from RFP was found to be approximately 1000 times stronger than luciferase²¹. The weak signal from luciferase necessitates photon counting, with the construction of a pseudo-image *in vivo* rather than true imaging, therefore greatly reducing resolution and precluding the *in vivo* cellular imaging that is an important feature of GFP imaging. In addition, the rapid clearance of the injected luciferase results in an unstable signal that makes comparison of data difficult²². The stronger signals from fluorescent proteins allow much more cost-efficient instrumentation. To overcome limits on fluorescent protein imaging imposed by the skin, reversible skin-flap window models have been developed that allow single-cell imaging on most organs of the mouse²³. The main advantage of luciferase-based imaging is that no excitation light is required, unlike fluorescence imaging. This feature of luciferase-based imaging could allow deeper imaging than with fluorescence, because excitation light is scattered and attenuated as it goes through skin, body tissues and fluids. See **Table 1** for a comparison of GFP and luciferase imaging.

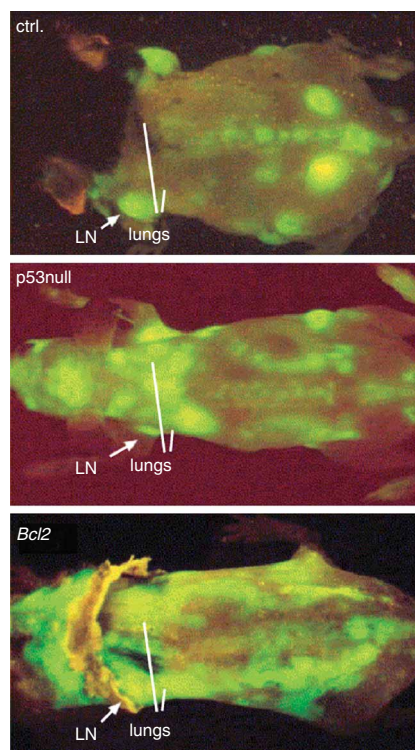


Figure 2 | Whole-body fluorescence imaging allows the visualization of lymphoma dissemination. At comparable lymph node (LN) enlargements (e.g., axillar LN, see arrows), *p53*-null and *Bcl2*-overexpressing lymphomas are much more disseminated, infiltrating liver, kidneys, lungs (marked) and brain, whereas the control (ctrl.) murine stem cell virus-based retroviral vectors (MSCV) lymphoma is restricted to the lymphoid compartment²⁴.

MATERIALS

REAGENTS

- Immunocompetent and immunodeficient mice (Charles River; Taconic; Harlan Teklad; see REAGENT SETUP)
- Cell lines, such as those derived from human cancer, to be transfected with genes coding for fluorescent proteins (American Type Culture Collection (ATCC))
- *Enhanced GFP* gene (Clontech Laboratories, Inc.)
- RFP (*DsRed2*) gene (Clontech Laboratories, Inc.)
- Retroviral vector pLEIN (Clontech Laboratories, Inc.)
- Retroviral vector pLNCX (Clontech Laboratories, Inc.)
- Retroviral pLACX vector (Clontech Laboratories, Inc.)
- Retroviral pFB-GFP vector (Clontech Laboratories, Inc.)
- vAd-GFP (Quantum)
- Supernatants of PT67-GFP cells, PT67-RFP cells, PT67 H2B-GFP cells (Clontech Laboratories Inc.)
- Growth medium (normal and selective), appropriate for cell culture (Life Technologies)
- HEPES buffer (20 mM, pH 7.2; Sigma)
- DOTAB reagent (Boehringer)
- LipofectAMINE Plus (Life Technologies)
- Cloning cylinders (Bel-Art Products)
- Anesthetic reagents (ketamine, xylazine, acepromazine maleate, isoflurane) (Butler Animal Health Supply)
- Nair (Carter-Wallace)
- G418 Neomycin (Life Technologies)
- PT67 packaging cells (Clontech Laboratories Inc.)

EQUIPMENT

- OV100 Small Animal Imaging System (Olympus Corp.)
- Leica fluorescence stereo microscope model LZ12 (Leica)
- Leica MZ6 stereo microscope (Nussloch)

- Hamamatsu C5810 three-chip cooled color CCD camera (Hamamatsu Photonics Systems)
- Lighttools Fluorescent Imaging System (Lighttools Research)
- Sony VCR model SLV-R1000 (Sony Corp.)
- Image Pro Plus 4.0 software (Media Cybernetics)
- 1 ml 27G2 latex-free syringe (Becton Dickinson)
- 25 μ l Hamilton syringe (Fisher Scientific)
- Humidified incubator with an atmosphere of 5% CO₂ (Hotpack)
- Blue LED flashlight (LDP LLC)
- D470/40 excitation filter (Chroma Technology)
- GG475 emission filter (Chroma Technology)
- Culture dishes, including 6-well and 96-well dishes (Fisher Scientific)
- Cloning cylinders (Bel-Art Products)
- Lipofectamine Plus transfection kit (Life Science)

REAGENT SETUP

Immunocompetent and immunodeficient mice **! CAUTION** All animal studies are conducted in accordance with the principles and procedures outlined in the National Institutes of Health National Research Council's *Guide for the Care and Use of Laboratory Animals* (available at <http://www.nap.edu/readingroom/>) under assurance number A3873-1. Animals are kept in a barrier facility under high-efficiency particulate air (HEPA) filtration. Mice are fed with autoclaved laboratory rodent diet (Teklad LM-485, Western Research Products).

Retroviral pLACX vector **! CAUTION** The National Institutes of Health and Center for Disease Control have designated retroviruses as Level 2 organisms. This requires the maintenance of a Biosafety Level 2 facility, including performing the work in a limited-access area, posting biohazard warning signs, minimizing the production of aerosols, decontaminating potentially infectious waste before disposal and taking precautions with sharps. For more information on Biosafety Level 2, see the following reference: *Biosafety in Microbiological and*

Biomedical Laboratories, 3rd Edn HHS Pub. #(CDC) 93-8395 (U.S. Department of Health and Human Services, PHS, CDC, NIH, 1993)

EQUIPMENT SETUP

Whole-body imaging equipment Use an Olympus OV100 Small Animal Imaging System, containing an MT-20 light source (Olympus Biosystems) and DP70 CCD camera (Olympus), for whole-body imaging in live mice at variable magnification. The optics of the OV100 fluorescence imaging system have been specially developed for macroimaging as well as microimaging, with high light-gathering capacity. The instrument incorporates a unique combination of high numerical aperture and long working distance. Five individually optimized objective lenses, parcentered and parfocal, provide a 10⁵-fold magnification range for seamless imaging of the entire body down to the subcellular level without disturbing the animal. The OV100 has the lenses mounted on an automated turret with a high magnification range of ×1.6 to ×16 and a field of view ranging from 6.9–0.69 mm. The optics and antireflective coatings ensure optimal imaging of multiplexed fluorescent reporters in small animals.

High-resolution images are captured directly on a PC (Fujitsu Siemens, Celsius W340, Model MTR-D2156). An equivalent model can also be used. Images are processed for contrast and brightness and analyzed with the use of Paint Shop Pro 8 (Corel Corp.) and Cell (Olympus Biosystems).

Many other fluorescence imaging systems can also be used for dual-color tumor–host imaging. For example, a Leica fluorescence stereo microscope (model LZ12) equipped with a mercury 50-W lamp power supply can be used. Selective excitation of GFP is produced through a D425/60 band-pass filter and 470 DCXR dichroic mirror. Emitted fluorescence is collected through a long-pass filter (GG475). Under anesthesia, the experimental

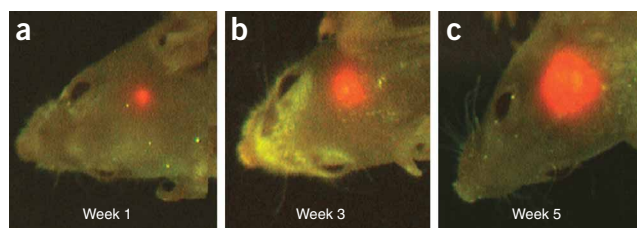


Figure 3 | Whole-body imaging of a brain tumor. Real-time whole-body imaging of a U87-GFP human glioma growing in the brain of a nude mouse at (a) 1 week, (b) 3 weeks and (c) 5 weeks after surgical orthotopic implantation⁵.

animals can be examined with the microscope and the images can be acquired with a Hamamatsu C5810 three-chip cooled color CCD camera. Images can also be processed for contrast and brightness and analyzed with the use of Image Pro Plus software. High-resolution images of 1,024 × 724 pixels can be captured directly on a computer or continuously through video output on a high-resolution Sony VCR, model SLV-R1000 (Sony Corp.).

Simpler systems such as a light box with appropriate filters and camera or even a blue light LED flashlight with appropriate filters can be used for macroimaging (see below).

PROCEDURE

GFP retrovirus production

- 1| For a GFP expression vector, use the pLEIN or equivalent retroviral vector expressing enhanced GFP and the neomycin resistance gene on the same bicistronic message.
- 2| Use PT67, an NIH3T3-derived packaging cell line, expressing the 10 A1 viral envelope to produce retrovirus. Culture PT67 cells in DMEM medium supplemented with 10% (vol/vol) heat-inactivated FCS. It takes approximately 3 d for the cells to reach ~70% confluence after seeding of 3 × 10⁵ PT67 cells in a 25 mm² flask with DMEM medium containing 10% FCS.
- 3| For vector production, use PT67 packaging cells, at 70% confluence. Plate PT67 cells on a 60-mm dish at 60–80% confluence 12 h before transfection. Use 10 μg of pFB-GFP with the Lipofectamine Plus transfection kit. Add 7 μl of pre-complexed pFB-GFP DNA in 87 μl of serum-free medium and then add 6 μl Lipofectamine reagent in a tube; mix and incubate at room temperature (22–26 °C) for 15 min.
- 4| Dilute 4 μl of Lipofectamine in 96 μl serum-free medium in a second tube. Mix and incubate at room temperature for 15 min.
- 5| Combine pre-complexed DNA and diluted Lipofectamine reagent; then mix and incubate at room temperature for 15 min.
- 6| While the complexes are forming, replace medium on the cells with 800 μl serum-free DMEM. Add the DNA–Lipofectamine reagent complex to the dish with cells containing fresh DMEM. Mix the complexes into the medium gently; incubate at 37 °C, 5% CO₂ for 4 h.
- 7| After 4 h incubation, increase volume of medium to 5 ml. Incubate at 37 °C, 5% CO₂ for 24 h.
- 8| After 24 h incubation, clone the packaging cells by limit dilution in 96-well plates where cells are plated to a density of less than one cell per well.

TABLE 1 | Comparison of optical imaging methods for tumor growth and metastasis²⁸.

Parameter	GFP/RFP	Luciferase	Reference
Strength of signal	6.6 × 10 ⁹ pixels s ⁻¹ cm ⁻² steradian ⁻¹	7.4 × 10 ⁶ pixels s ⁻¹ cm ⁻² steradian ⁻¹	21
Minimum number of cells imageable <i>in vitro</i>	1	300	29,30
Minimum number of cells imageable <i>in vivo</i>	1	3,000	23,29,31,32
Need for substrate	No	Yes	23,29,32
Need for anesthesia	No	Yes	23,32
Method of visualization	Direct imaging	Photon-counting (pseudo-image)	1,32
Multi-color imaging	Yes	No	23
Stability of signal	Yes	No	6,22
Need for excitation light	Yes	No	6,32



PROTOCOL

9| Examine the cells by fluorescence microscopy 48 h post-transduction.

10| For selection, culture the cells in the presence of 300, 400, 500–2000 $\mu\text{g ml}^{-1}$ G418, increased in a stepwise manner, to select for a clone producing high amounts of a GFP retroviral vector (PT67-GFP). Culture the cells for 1–2 days in each concentration of G418. High-viral-titer production clones of GFP PT67 cells are identified with 3T3 cells used for virus titering. Clones with titer higher than 10^6 plaque-forming units (pfu) are used for GFP vector production.

▲ **CRITICAL STEP** Increasing the level of G418 in a stepwise manner is very important to induce the expression of the transgene. This procedure assures high-level production of GFP retrovirus.

RFP retrovirus production

11| Insert the *HindIII/NotI* fragment from pDsRed2, containing the full-length red fluorescent protein cDNA, into the *HindIII/NotI* site of pLNCX2 that has the neomycin resistance gene to establish the pLNCX2-DsRed2 plasmid.

12| Incubate PT67 cells at 70% confluence for 24 h at 37 °C. Lipofectamine reagent is used as described in Steps 3–8 to transfect the pLNCX2-DsRed2 vector into the PT67 cells.

13| Culture the cells in the presence of 200–1000 $\mu\text{g ml}^{-1}$ of G418 to select a clone producing high amounts of RFP retroviral vector (PT67-DsRed2). Culture the cells for 1–2 d in each concentration of G418 in step-wise increases of 100 $\mu\text{g ml}^{-1}$.

▲ **CRITICAL STEP** This procedure assures high-level production of RFP retrovirus as described in Step 10.

Production of histone H2B-GFP vector

14| Insert the histone *H2B-GFP* fusion gene at the *HindIII/ClaI* site of the pLHCX retrovirus that has the hygromycin resistance gene.

15| To establish a packaging cell clone producing high amounts of a histone H2B-GFP retroviral vector, transfect the pLHCX histone H2B-GFP plasmid in PT67 cells using the same methods described above for PT67-DsRed2 (Step 12).

16| Culture the transfected cells in the presence of 200–400 $\mu\text{g ml}^{-1}$ hygromycin to establish stable PT67 H2B-GFP packaging cells. The amount of hygromycin is increased stepwise as described above for G418.

▲ **CRITICAL STEP** This procedure assures high-level production of histone H2B-GFP retrovirus.

RFP or GFP gene transduction of tumor cell lines

17| For RFP or GFP gene transduction, use 20% confluent cancer cells. 12–18 h before infection with GFP or RFP retrovirus, plate the target cells at a cell density of $1-2 \times 10^5$ per 60 mm plate.

18| For retroviral infection, collect conditioned medium from packaging cells (PT67/pFB GFP or PT67/pLNCX2-DsRed2) and filter medium through a 0.45 μm polysulfonic filter. Add virus-containing filtered medium to target cells. Add polybrene to a final concentration of 8 $\mu\text{g ml}^{-1}$. Incubate cells for 24 h at 37 °C.

19| Replace medium with DMEM and 10% (vol/vol) FCS after 24 h incubation.

20| Check for GFP- or RFP-expressing cells by fluorescence microscopy.

21| Harvest tumor cells with trypsin/EDTA and subculture them at a ratio of 1:15 in a selective medium that contains 50 $\mu\text{g ml}^{-1}$ of G418.

22| To select brightly fluorescent cells, increase the level of G418 to 800 $\mu\text{g ml}^{-1}$ in a stepwise manner. Culture the cells for 1–2 d in each concentration of G418, using at least four different concentrations.

▲ **CRITICAL STEP** Increasing the level of G418 in a stepwise manner is very important to induce the expression of the transgene. This procedure ensures high-level production of GFP or RFP in the cells.

23| Isolate clones expressing GFP or RFP with cloning cylinders by trypsin/EDTA and amplify them in DMEM and 10% FCS in the absence of selective agent. Further select cells for brightness and stability.

▲ **CRITICAL STEP** This step ensures that the cells will stably express GFP or RFP in the absence of antibiotic selection, which is the case *in vivo*.

Double RFP and histone H2B-GFP gene transduction of cancer cells

24| To establish dual-color cancer cells, use clones of cancer cells expressing RFP in the cytoplasm at 70% confluence. Incubate RFP cancer cells, produced as described above (Steps 17–23), with the retroviral-containing medium supernatants of PT67 H2B-GFP cells and the above culture medium for 48 h at 37 °C. To obtain the double transformants, incubate cells with hygromycin 48 h after transfection and select as described above (Step 16).

Establishment of imageable tumor models

25| A number of options are available for establishing tumor models using fluorescent protein-expressing tumor cells, including cell injection, surgical orthotopic implantation and DNA expression models of organs.

(A) Cell injection to establish experimental metastasis model

- (i) Harvest fluorescent protein-expressing tumor cells by trypsinization using 0.25% (wt/vol) trypsin for 3 min at 37 °C.
- (ii) Wash cells three times with cold serum-free medium using a tabletop centrifuge at 2,000 rpm for 5 min at room temperature.
- (iii) Resuspend the cells in approximately 0.2 ml of serum-free medium.
- (iv) Within 30 min of harvesting, inject 6-week-old GFP-C57CL/6 or nude (*nu/nu*) GFP mice with 10^6 tumor cells into the lateral tail vein or subcutaneously, in a total volume of 0.2 ml using a 1 ml 27G2 latex-free syringe.
 - ▲ **CRITICAL STEP** Cells in suspension can lose viability over time and therefore should be injected as soon as possible.
- (v) For liver colonization, inject fluorescent protein-expressing cells directly into the portal vein under anesthesia (please see below for details on inducing anesthesia).

(B) Subcutaneous injection of cancer cells

- (i) Collect cancer cells by trypsinization with 0.25% trypsin for 3 min at 37 °C.
- (ii) Wash cells three times with cold serum-containing medium using a tabletop centrifuge at 500g for 5 min at room temperature, and then keep on ice.
- (iii) Inject 6-week-old GFP male C57BL/6 or GFP nude mice subcutaneously with 1×10^6 cancer cells that were collected and washed. This is done by inoculating cells by subcutaneous injection of the dorsal skin of the mouse in a total volume of 50 μ l of cell culture medium within 40 min of collection.

(C) Surgical orthotopic implantation (SOI) to establish spontaneous metastasis model

- (i) Induce anesthesia with ketamine mixture (10 μ l ketamine HCL, 7.6 μ l xylazine, 2.4 μ l acepromazine maleate and inject subcutaneously).
- (ii) Perform all procedures of the operation under a $\times 7$ magnification microscope (Leica MZ6).
- (iii) Isolate fluorescent protein-expressing tumor fragments (1 mm³) from subcutaneously growing tumors, which were formed from injected RFP- or GFP-expressing tumor cells (see Step 17), by mincing tumor tissue. After proper exposure of the target organ, implant three tumor fragments per mouse.
- (iv) Using an 8-0 surgical suture, penetrate the tumor fragments and suture the fragments onto the target organ.
 - ▲ **CRITICAL STEP** Orthotopic implantation of tumor fragments results in higher spontaneous metastatic rates than injection of a cell suspension.
- (v) Keep animals in a barrier facility under HEPA filtration.

(D) Using the footpad to establish an imageable angiogenesis model

- (i) Subcutaneously inject cancer that stably expresses GFP into the footpad of 6-week-old nude mice.

(E) Imageable gene expression models

- (i) For the DNA expression models, *vAd-GFP* is delivered to various organs for subsequent whole-body imaging.

(F) DNA expression model in the brain

- (i) Induce anesthesia with the ketamine mixture as described above.
- (ii) Make an upper midline scalp incision to expose the parietal bone of the skull.
 - ▲ **CRITICAL STEP** This step and all subsequent steps should be performed with a $\times 7$ magnification stereo microscope (Leica MZ12).
- (iii) Inject 20 μ l of recombinant adenovirus in phosphate-buffered saline (PBS) with 10% (vol/vol) glycerol containing 8×10^{10} pfu ml⁻¹ of vAd-GFP per mouse into the skull using a 1 ml 27G1/2 latex-free syringe.
 - ▲ **CRITICAL STEP** Plug the puncture hole in the skull with bone wax in order to seal the skull.
- (iv) Close the incision in the scalp with a 7-0 surgical suture in one layer.

(G) DNA expression model in the liver

- (i) Induce anesthesia with the ketamine mixture as described above.
- (ii) Make an upper midline abdominal incision to expose the portal vein.
 - ▲ **CRITICAL STEP** This step and all subsequent steps should be performed with a $\times 7$ magnification stereo microscope (Leica MZ12).
- (iii) Inject 100 μ l of PBS with 10% glycerol containing 8×10^{10} pfu ml⁻¹ vAd-GFP per mouse into the portal vein using a 1 ml 39G1 latex-free syringe.
 - ▲ **CRITICAL STEP** For hemostasis, press the puncture hole in the portal vein with sterile cotton for about 10 seconds in order to prevent excess blood loss.
- (iv) Close the incision in the abdominal wall with a 7-0 surgical suture in one layer.

(H) DNA expression model in the pancreas

- (i) Induce anesthesia with the ketamine mixture as described above.
- (ii) Make an upper midline abdominal incision to expose the pancreas.

PROTOCOL

▲ **CRITICAL STEP** This step and all subsequent steps should be performed with a $\times 7$ magnification stereo microscope (Leica MZ12).

(iii) Inject 100 μl of PBS with 10% glycerol containing 8×10^{10} pfu ml^{-1} vAd-GFP per mouse into the pancreas using a 1 ml 39G1 latex-free syringe.

▲ **CRITICAL STEP** Press the puncture hole for about 10 seconds with sterile cotton for hemostasis in order to prevent excess blood loss.

(iv) Close the incision with a 7-0 surgical suture in one layer.

(I) DNA expression model in the prostate

(i) Induce anesthesia with the ketamine mixture as described above.

(ii) Make a lower midline abdominal incision to expose the bladder and prostate.

▲ **CRITICAL STEP** This step and all subsequent steps should be performed with a $\times 7$ magnification stereo microscope (Leica MZ12).

(iii) Inject 30 μl of PBS with 10% glycerol containing 8×10^{10} pfu ml^{-1} vAd-GFP per mouse in the prostate using a 1-ml 39G1 latex-free syringe.

▲ **CRITICAL STEP** Press the puncture hole in the prostate for about 10 seconds with sterile cotton for hemostasis in order to prevent excess blood loss.

(iv) Close the incision with a 6-0 surgical suture in one layer.

(J) DNA expression model in the bone marrow

(i) Induce anesthesia with the ketamine mixture as described above.

(ii) Open the skin on the hind leg with a 1-cm incision to expose the tibia.

▲ **CRITICAL STEP** This step and all subsequent steps should be performed with a $\times 7$ magnification stereo microscope (Leica MZ12).

(iii) Insert a 27-gauge needle with a latex-free syringe in the bone marrow cavity.

(iv) Inject a total volume of 20 μl of PBS with 10% glycerol (8×10^{10} pfu/ml) vAd-GFP per mouse into the bone marrow cavity.

▲ **CRITICAL STEP** Plug the puncture hole in the bone with bone wax and close the incision with a 6-0 surgical suture in order to seal the bone.

26 | A number of methods are available for whole-body imaging of mice, including chamber, microscopy, flashlight imaging and light-box imaging.

(A) Whole-body imaging with a microscope

(i) Use a Leica fluorescence stereo microscope (model LZ12) equipped with a mercury 50 W lamp power supply or equivalent.

(ii) Produce selective excitation of GFP through a D425/60 band-pass filter and 470 DCXR dichroic mirror.

(iii) Collect emitted fluorescence through a long-pass filter (GG475) on a Hamamatsu C5810 three-chip cooled color CCD camera or equivalent.

(iv) Process images for contrast and brightness with the use of Image Pro Plus 4.0 software or equivalent.

(v) Capture high-resolution images of $1,024 \times 724$ pixels directly on an IBM PC or continuously through video output on a high-resolution Sony VCR, model SLV-R1000 or equivalent.

(vi) In the case of C57BL/6 mice, remove hair with depilatory cream (e.g., Nair) or by shaving.

▲ **CRITICAL STEP** Hair is highly autofluorescent, so improper removal of hair will result in low-quality images.

(B) Whole-body imaging with a flashlight

(i) Use a blue LED flashlight with an excitation filter (midpoint wavelength peak of 470 nm) and a D470/40 emission filter for whole-body imaging of RFP- or GFP-expressing mice with RFP-expressing tumors growing in or on internal organs.

▲ **CRITICAL STEP** Correct filters are necessary to eliminate tissue autofluorescence.

(ii) Acquire images with a digital camera such as a Nikon Cool-PIX or a simple CCD camera and store on a PC as described above.

(iii) In the case of C57BL/6 mice, remove hair with depilatory cream or by shaving.

▲ **CRITICAL STEP** Hair is highly autofluorescent, so improper removal of hair will result in low-quality images.

(C) Whole-body imaging in a light box

(i) Perform whole-body imaging in a fluorescent light box illuminated by fiberoptic lighting at 470 nm.

(ii) Collect emitted fluorescence through a GG475 long-pass filter on a Hamamatsu C5810 three-chip cooled color CCD camera or equivalent (use of separate band-pass filters for RFP or GFP emission allows a monochrome camera to be used).

(iii) Capture high-resolution images of $1,024 \times 724$ pixels directly on an IBM PC or equivalent.

(iv) Process images for contrast and brightness with the use of Image Pro Plus 4.0 software or equivalent.

(v) In the case of C57BL/6 mice, remove hair with depilatory cream or by shaving.

▲ **CRITICAL STEP** Hair is highly autofluorescent, so improper removal of hair will result in low-quality images.

(D) Whole-body imaging in a chamber

(i) Perform whole-body imaging in an Olympus OV100 imaging system with 470 nm excitation light originating from an MT-20 light source.

BOX 1 | IMAGE ANALYSIS

Measuring the intensity of GFP images of internally growing tumors and *in vivo* gene expression is carried out as described below. Image size can be analyzed by using Image Pro Plus or Adobe Photo shop. The pixel area of the image is determined and converted to mm². It should be noted that image area and actual volume have been shown to correlate for tumors³.

Steps for quantification of image size

- Open the image file with Image Pro Plus, use the manual measurement function and then mark the periphery around the image.
- Make measurements by clicking on the area icon or double-click on indicated length.
- Export the data to Microsoft Excel for statistical analysis

Measuring the intensity of GFP expression

The ratio of GFP to intrinsic red fluorescence intensity of the skin is a reliable and convenient index for analyzing and quantifying the intensity of a GFP image. A ratio (γ) of green to red channels in a color CCD camera can be determined for each pixel in the image with and without GFP. Values of γ for mouse skin in the absence of GFP vary between 0.7 and 1.0. The intensity of GFP fluorescence can then be determined by subtracting the intrinsic value of γ from that obtained from the GFP image. The integral of GFP fluorescence intensity above the intrinsic maximum value of γ for skin without GFP can then be obtained by making the determination for each pixel in the image.

Steps for quantification of intensity

- Open the image file with Image Pro Plus software and use the icon to outline the area of interest, and then mark the area of interest either automatically or manually.
- Open image histogram and then read the intensity of green or red channels to obtain the values for γ as outlined above for each pixel, and multiply by the number of pixels to obtain the total intensity.
- Export the data to Microsoft Excel for statistical analysis.

It should be noted that image attenuation will occur as a function of depth. Such attenuation can be estimated by comparing the area of the whole-body image to that of the intravital image in the opened animal. An example of such a comparison is shown in **Figure 9**, demonstrating that attenuation, even for a GFP tumor on the colon, is moderate²⁷ (see **Table 3**).

- (ii) Collect emitted fluorescence through appropriate filters configured on a filter wheel with a DP70 CCD camera. Variable magnification imaging can be performed with a series of five objective lenses.
- (iii) Capture images on a PC, and process images for contrast and brightness with Paint Shop Pro 8 and Cell^R.
- (iv) In the case of C57BL/6 mice, remove hair with depilatory cream or by shaving.
 - ▲ **CRITICAL STEP** Hair is highly autofluorescent, so improper removal of hair will result in low-quality images.

27| Analyse the obtained images (**Box 1** and **Table 3**).

● TIMING

- Steps 1–10: 2 weeks
- Steps 11–13: 2 weeks
- Steps 14–16: 2 weeks
- Steps 17–23: 7–10 days
- Step 24: 4–8 weeks
- Step 25(A): 2–4 weeks
- Step 25(B): 4 weeks
- Step 25(C): 2–8 weeks
- Steps 25(D): 1–2 weeks
- Steps 25(E–J): 1–2 days
- Step 26: 1–3 hours
- Step 27: 1–3 hours

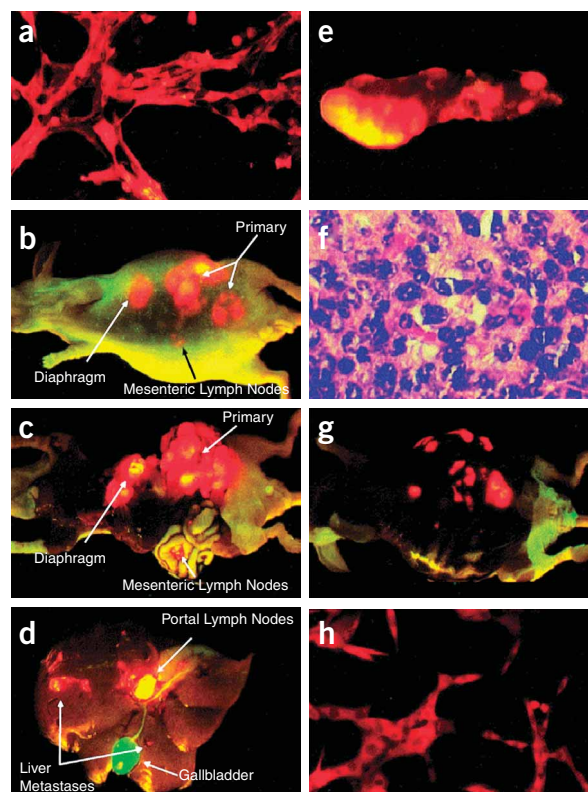


Figure 4 | Correlation of whole-body and open images. (a) High-level expression of red fluorescent protein (RFP) in MIA-PaCa-2 cells *in vitro*. (b) External and (c) open images of a single, representative control mouse at autopsy on day 17 after surgical orthotopic implantation. A strong correlation can be observed between the fluorescence visualized externally and that obtained after laparotomy is evident. (d) The liver, (e) spleen, and other solid organs were removed at autopsy and examined for evidence of metastatic disease. (f) Hematoxylin and eosin staining. (g) Intra-abdominal ascites. (h) Colonies of MIA-PaCa-2-RFP clones were easily retrieved and cultured from this aspirated ascites fluid³.

PROTOCOL

? TROUBLESHOOTING

Troubleshooting guidance can be found in **Table 2**.

TABLE 2 | Troubleshooting table.

Problem	Possible reason	Solution
Autofluorescence	Use of wrong filters	It is important to minimize autofluorescence of the tissue and body fluids by using proper filters. Excitation filters should have a narrow band as close to 490 nm as possible to specifically excite GFP whose peak is distinct from that of the skin, tissues and fluid of the animal. In addition, proper band-pass emission filters should be used with a cut-off of approximately 515 nm.
Bleeding	Improper surgical procedures	Bleeding should be avoided at the surgical site as hemoglobin will absorb the incident excitation light.
Dehydration	Long-term procedures on an open animal	When using open-biopsy procedures, it is essential to hydrate the animal by spraying normal saline on the open tissue.
Infection	Unclean instruments and environment	When using repeat procedures such as an open biopsy or other invasive procedures, it is crucial to maintain a proper sterile operation field.

ANTICIPATED RESULTS

The procedures described in this protocol enable whole-body imaging of fluorescent cells in essentially any organ. Examples include **Figure 1**, which shows whole-body imaging of GFP-labeled cancer cells in the liver and skull¹. **Figure 2** is an example of 'molecular imaging', with whole-body images of a mouse lymphoma arising from a transgenic *Eμ-Myc* mouse. The virulence of the tumor is determined by genes controlling apoptosis such as *p53* and *BCL2*. Fluorescent tumor cells can be whole-body imaged in numerous lymphatic and non-lymphatic organs²⁴. **Figure 3** demonstrates the use of red fluorescent protein (DsRed2). In this case, human glioma

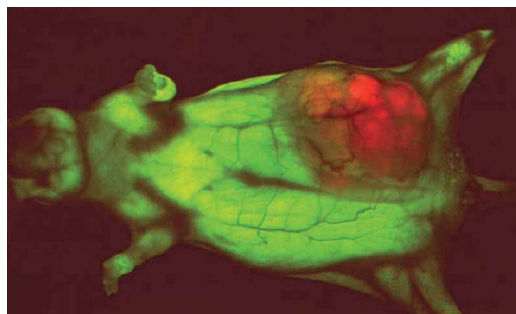


Figure 5 | Whole-body image of orthotopically growing human colon tumor 116-RFP human colon cancer in GFP nude mouse²⁵.

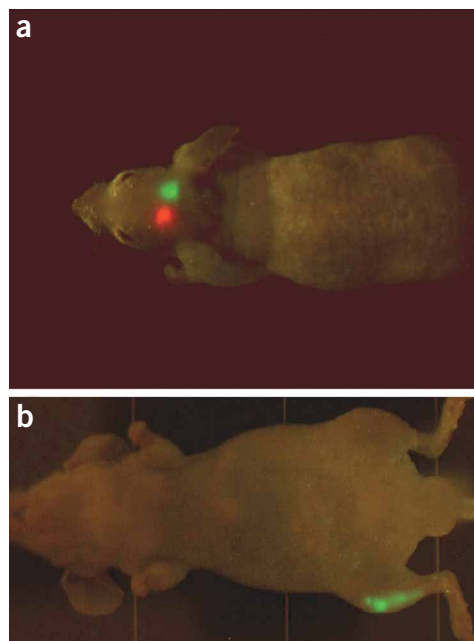


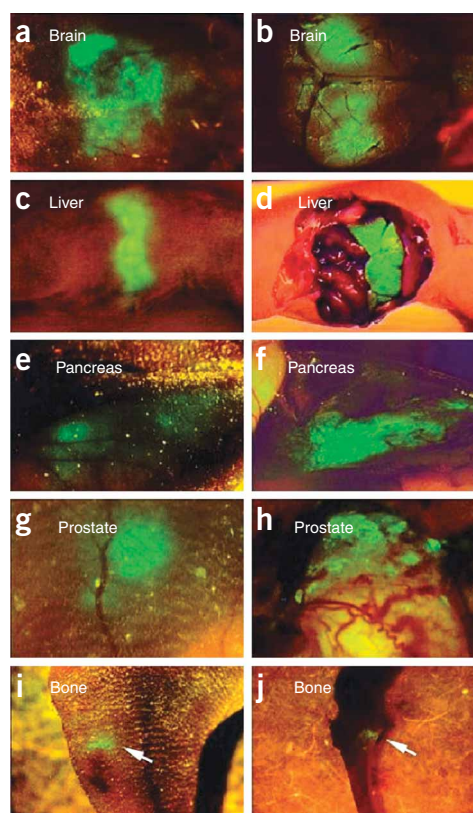
Figure 6 | Whole-body imaging with an LED flashlight. (a) GFP- and RFP-expressing tumors implanted in the brain in a single nude mouse. The excitation light was produced with a simple blue-LED flashlight equipped with an excitation filter with a central peak of 470 nm. (b) GFP-expressing tumor implanted in the tibia of the right hind leg of a nude mouse imaged with the blue-LED flashlight as in panel A (ref. 27).

TABLE 3 | Comparison of whole-body and intravital open images.

Tumor location	Number of pixels in image	Area of the image (mm ²)
GFP colon (whole-body image)	2,465	16.22
GFP colon (intravital image)	2,731	17.97



Figure 7 | External and internal images of *vAd-GFP* gene expression in various organs. Series of external fluorescence images of *vAd-GFP* gene expression in the brain, liver, pancreas, prostate and tibia (**a, c, e, g and i**), compared with corresponding images of the exposed organs (**b, d, f, h and j**)¹⁰.



U87 is implanted in the brain of nude mice and whole-body imaging⁵ demonstrates growth of the tumor over a five-week period. **Figure 4** demonstrates whole-body imaging of a highly metastatic pancreatic cancer expressing RFP compared to open imaging of the same tumor. Comparison of the two-dimensional image with the measured volume of the tumor in the opened animal results in a straight line ($r = 0.89$). These results demonstrate that the easily acquired whole-body images correlate with tumor volume, thereby validating the imaging method for studying tumor growth and the efficacy of anti-tumor drugs³. **Figure 5** is an example of a whole-body image of an RFP-expressing human colon tumor HCT-116 orthotopically implanted in a ubiquitously expressing GFP mouse. Dual-color models are highly suitable to study tumor-host interaction, as all tumor cells will fluoresce red and all normal cells will fluoresce green²⁵. **Figure 6** shows that a simple blue LED flashlight with an excitation filter and emission filter can be used to obtain very bright whole-body

images of fluorescent cancer cells on internal organs. In this case, a GFP and an RFP tumor are simultaneously imaged and a GFP tumor in the tibia is imaged in another animal. Note the lack of autofluorescence detected in the skin⁵. **Figure 7** is an example of whole-body imaging of gene expression using GFP. In this case, GFP is linked to an adenovirus which was injected into various organs. Whole-body images of adenoviral GFP expression in the brain, liver, pancreas, prostate and bone are compared with open imaging¹⁰. **Figure 8** is an example of a state-of-the-art imaging system, the Olympus OV100 (ref. 26). This system enables whole-body imaging as described above as well as subcellular imaging of cancer cells, which is detailed in another protocol¹². The signal from fluorescent protein imaging is so strong that open and whole-body images are comparable. For example, **Figure 9** shows whole-body and open images of a GFP-expressing tumor on the colon with only moderate attenuation of the signal in the whole-body image.

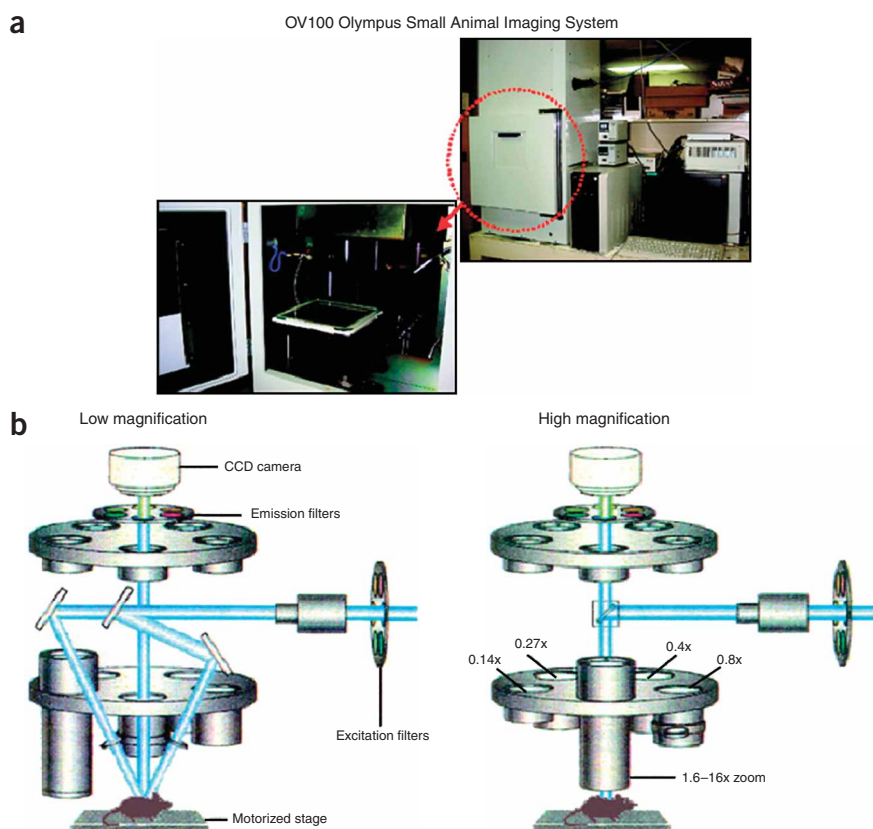


Figure 8 | Variable magnification whole-animal imaging system. (a) Olympus OV100 Small Animal Imaging System. See main text for details. (b) OV100 covers a wide range of magnifications, from $\times 0.14$ (63×47 mm imaging area) to $\times 16$ (0.6×0.45 mm)²⁶.

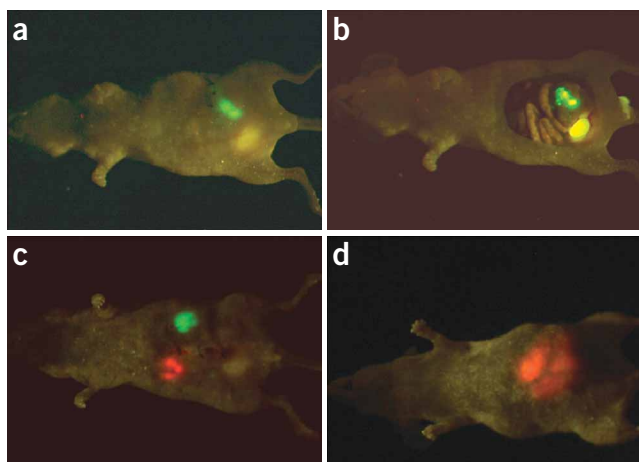


Figure 9 | Whole-body and open imaging of GFP and RFP tumors in nude mice. (a) Whole-body imaging shows the GFP-expressing tumor on the colon imaged with the blue-LED flashlight. (b) Same as a, with animal opened. (c) Image of RFP-expressing tumor on the liver and GFP-expressing tumor on the pancreas in a nude mouse. The tumors were imaged with the blue-LED flashlight. (d) Whole-body image of a metastasizing RFP-tumor on the pancreas in a nude mouse²⁶.

The future is bright for applications of this powerful technology, which will provide new visible targets for novel drugs and will enable cell biology to be studied in the live animal.

COMPETING INTERESTS STATEMENT The authors declare competing financial interests (see the HTML version of this article for details).

Published online at <http://www.natureprotocols.com>
 Reprints and permissions information is available online at <http://npg.nature.com/reprintsandpermissions>

1. Yang, M. *et al.* Whole-body optical imaging of green fluorescent protein-expressing tumors and metastases. *Proc. Natl. Acad. Sci. USA* **97**, 1206–1211 (2000).
2. Yang, M. *et al.* Real-time whole-body imaging of an orthotopic metastatic prostate cancer model expressing red fluorescent protein. *Prostate* **62**, 374–379 (2005).
3. Katz, M.H. *et al.* A novel red fluorescent protein orthotopic pancreatic cancer model for the preclinical evaluation of chemotherapeutics. *J. Surg. Res.* **113**, 151–160 (2003).
4. Peyruchaud, O. *et al.* Early detection of bone metastases in a murine model using fluorescent human breast cancer cells: application to the use of the bisphosphonate zoledronic acid in the treatment of osteolytic lesions. *J. Bone Miner. Res.* **16**, 2027–2034 (2001).
5. Hoffman, R.M. Green fluorescent protein imaging of tumor cells in mice. *Lab Anim.* **31**, 34–41 (2002).
6. Hoffman, R.M. The multiple uses of fluorescent proteins to visualize cancer *in vivo*. *Nature Rev. Cancer* **5**, 796–806 (2005).
7. Yang, M. *et al.* Whole-body and intravital optical imaging of angiogenesis in orthotopically implanted tumors. *Proc. Natl. Acad. Sci. USA* **98**, 2616–2621 (2001).
8. Hemann, M.T. *et al.* Evasion of the p53 tumour surveillance network by tumour-derived MYC mutants. *Nature* **436**, 807–811 (2005).
9. Mitsiades, C.S. *et al.* Fluorescence imaging of multiple myeloma cells in a clinically relevant SCID/NOD *in vivo* model: biologic and clinical implications. *Cancer Res.* **63**, 6689–6696 (2003).
10. Yang, M., Baranov, E., Moossa, A.R., Penman, S. & Hoffman, R.M. Visualizing gene expression by whole-body fluorescence imaging. *Proc. Natl. Acad. Sci. USA* **97**, 12278–12282 (2000).
11. Panoskaltsis-Mortari, A. *et al.* *In vivo* imaging of graft-versus-host-disease in mice. *Blood* **103**, 3590–3598 (2004).
12. Zhao, M. *et al.* Spatial-temporal imaging of bacterial infection and antibiotic response in intact animals. *Proc. Natl. Acad. Sci. USA* **98**, 9814–9818 (2001).
13. Hoffman, R.M. & Yang, M. Subcellular imaging in the live mouse. *Nat. Protocols* **1**, 775–782 (2006).
14. Heim, R., Cubitt, A.B. & Tsien, R.Y. Improved green fluorescence. *Nature* **373**, 663–664 (1995).
15. Cormack, B., Valdivia, R. & Falkow, S. FACS-optimized mutants of the green fluorescent protein (GFP). *Gene* **173**, 33–38 (1996).

16. Cramer, A., Whitehorn, E.A., Tate, E. & Stemmer, W.P.C. Improved green fluorescent protein by molecular evolution using DNA shuffling. *Nature Biotechnol.* **14**, 315–319 (1996).
17. Delagrave, S., Hawtin, R.E., Silva, C.M., Yang, M.M. & Youvan, D.C. Red-shifted excitation mutants of the green fluorescent protein. *Bio/technology* **13**, 151–154 (1995).
18. Zolotukhin, S., Potter, M., Hauswirth, W.W., Guy, J. & Muzyczka, N. A ‘humanized’ green fluorescent protein cDNA adapted for high-level expression in mammalian cells. *J. Virol.* **70**, 4646–4654 (1996).
19. Martin, B.R., Giepmans, B.N., Adams, S.R. & Tsien, R.Y. Mammalian cell-based optimization of the biarsenical-binding tetracysteine motif for improved fluorescence and affinity. *Nature Biotechnol.* **23**, 1308–1314 (2005).
20. Cody, C.W., Prasher, D.C., Westler, V.M., Prendergast, F.G. & Ward, W.W. Chemical structure of the hexapeptide chromophore of the Aequorea green fluorescent protein. *Biochemistry* **32**, 1212–1218 (1993).
21. Ray, P., De, A., Min, J.-J., Tsien, R.Y. & Gambhir, S.S. Imaging tri-fusion multimodality reporter gene expression in living subjects. *Cancer Res.* **64**, 1323–1330 (2004).
22. Burgos, J.S. *et al.* Time course of bioluminescent signal in orthotopic and heterotopic brain tumors in nude mice. *Biotechniques* **34**, 1184–1188 (2003).
23. Yang, M. *et al.* Direct external imaging of nascent cancer, tumor progression, angiogenesis, and metastasis on internal organs in the fluorescent orthotopic model. *Proc. Natl. Acad. Sci. USA* **99**, 3824–3829 (2002).
24. Schmitt, C.A. *et al.* Dissecting p53 tumor suppressor functions *in vivo*. *Cancer Cell* **1**, 289–298 (2002).
25. Yang, M. *et al.* Dual-color fluorescence imaging distinguishes tumor cells from induced host angiogenic vessels and stromal cells. *Proc. Natl. Acad. Sci. USA* **100**, 14259–14262 (2003).
26. Yamauchi, K. *et al.* Development of real-time subcellular dynamic multicolor imaging of cancer-cell trafficking in live mice with a variable-magnification small animal imaging system. *Cancer Res.* **66**, 4208–4214 (2006).
27. Yang, M., Luiken, G., Baranov, E. & Hoffman, R.M. Facile whole-body imaging of internal fluorescent tumors in mice with an LED flashlight. *BioTechniques* **39**, 170–172 (2005).
28. Hoffman, R.M. Green fluorescent protein imaging of tumour growth, metastasis, and angiogenesis in mouse models. *Lancet Oncol.* **3**, 546–556 (2002).
29. Chishima, T. *et al.* Cancer invasion and micrometastasis visualized in live tissue by green fluorescent protein expression. *Cancer Res.* **57**, 2042–2047 (1997).
30. Dusich, J.M., Oei, Y.A., Purchio, T. & Jenkins, D.E. *In vivo* detection of lung colonization and metastasis using luciferase-expressing human A549 lung cells. *Proc. Am. Assoc. Cancer Res.* **43**, 1059 (2002).
31. Yamauchi, K. *et al.* Real-time *in vivo* dual-color imaging of intracapillary cancer cell and nucleus deformation and migration. *Cancer Res.* **65**, 4246–4252 (2005).
32. Vooijs, M., Jonkers, J., Lyons, S. & Berns, A. Noninvasive imaging of spontaneous retinoblastoma pathway-dependent tumors in mice. *Cancer Res.* **62**, 1862–1867 (2002).

